

Analytical Model for Fictitious Crack Propagation in Concrete Beams

Ulfkjær, J. P.; Krenk, S.; Brincker, Rune

Publication date:
1992

Document Version
Early version, also known as pre-print

[Link to publication from Aalborg University](#)

Citation for published version (APA):
Ulfkjær, J. P., Krenk, S., & Brincker, R. (1992). *Analytical Model for Fictitious Crack Propagation in Concrete Beams*. Dept. of Building Technology and Structural Engineering, Aalborg University. Fracture and Dynamics Vol. R9206 No. 34

General rights

Copyright and moral rights for the publications made accessible in the public portal are retained by the authors and/or other copyright owners and it is a condition of accessing publications that users recognise and abide by the legal requirements associated with these rights.

- Users may download and print one copy of any publication from the public portal for the purpose of private study or research.
- You may not further distribute the material or use it for any profit-making activity or commercial gain
- You may freely distribute the URL identifying the publication in the public portal -

Take down policy

If you believe that this document breaches copyright please contact us at vbn@aub.aau.dk providing details, and we will remove access to the work immediately and investigate your claim.

FRACTURE & DYNAMICS
PAPER NO. 34

Submitted to Journal of Engineering Mechanics

J. P. ULFKJÆR, S. KRENK & R. BRINCKER
ANALYTICAL MODEL FOR FICTITIOUS CRACK PROPAGATION IN
CONCRETE BEAMS
APRIL 1992

ISSN 0902-7513 R9206

The FRACTURE AND DYNAMICS papers are issued for early dissemination of research results from the Structural Fracture and Dynamics Group at the Department of Building Technology and Structural Engineering, University of Aalborg. These papers are generally submitted to scientific meetings, conferences or journals and should therefore not be widely distributed. Whenever possible reference should be given to the final publications (proceedings, journals, etc.) and not to the Fracture and Dynamics papers.

FRACTURE & DYNAMICS
PAPER NO. 34

Submitted to Journal of Engineering Mechanics

J. P. ULFKJÆR, S. KRENK & R. BRINCKER
ANALYTICAL MODEL FOR FICTITIOUS CRACK PROPAGATION IN
CONCRETE BEAMS
APRIL 1992

ISSN 0902-7513 R9206

Analytical Model for Fictitious Crack Propagation in Concrete Beams

By Jens Peder Ulfkjær¹, Steen Krenk² and Rune Brincker³

Abstract: An analytical model for load-displacement curves of unreinforced notched and un-notched concrete beams is presented. The load displacement-curve is obtained by combining two simple models. The fracture is modelled by a fictitious crack in an elastic layer around the mid-section of the beam. Outside the elastic layer the deformations are modelled by the Timoshenko beam theory. The state of stress in the elastic layer is assumed to depend bi-linearly on local elongation corresponding to a linear softening relation for the fictitious crack. For different beam size results from the analytical model are compared with results from a more accurate model based on numerical methods. The analytical model is shown to be in good agreement with the numerical results if the thickness of the elastic layer is taken as half the beam depth. Several general results are obtained. It is shown that the point on the load-displacement curve where the fictitious crack starts to develop, and the point where the real crack starts to grow will always correspond to the same bending moment. Closed form solutions for the maximum size of the fracture zone and the minimum slope on the load-displacement curve is given. The latter result is used for derivation of a general snap-back criterion depending only on beam geometry.

Introduction

Since Kaplan (Kaplan 1961) performed his linear elastic fracture mechanical (LEFM) investigation of notched concrete beams subjected to three and four point bending much attention has been paid to fracture of concrete and rock. In this pioneering work and in three subsequent discussions (Blakey and Beresford (1962), Glücklich (1962), Irwin (1962)) the applicability of LEFM was discussed and the views given in these contributions are still popular (e.g. slow crack growth). Today it is realized that LEFM is only applicable to large scale structures and ultra brittle concrete, Planas and Elices (1989), and that it is necessary to apply nonlinear fracture mechanics for description of fracture in ordinary concrete structures.

Different models based on nonlinear fracture mechanical ideas describe the softening behaviour of concrete e.g. the Fictitious Crack Model (FC-model) by Hillerborg, Modeer and Peterson (1976), the Crack Band model by Bazant (1983) and the Two Parameter Model by Jenq and Shah (1985). In this paper the FC-model will be used to describe fracture in concrete.

Few researchers have considered analytical methods based on non-linear elastic fracture mechanical models to describe fracture in concrete structures. A model has been developed by T. Chuang and Y.W. Mai (1989) based on the Crack Band Model. Also, a model based on the fictitious crack model has been developed by Llorca and Elices (1990).

The idea of modelling the bending failure of concrete beams by development of a fictitious crack in an elastic layer with a thickness proportional to the beam height was introduced by

¹ Res. Assistant, Dept. of Building Techn. and Struct. Engrg., University of Aalborg, Dk-9000 Aalborg, Denmark.

² Professor, Dept. of Building Techn. and Struct. Engrg., University of Aalborg.

³ Assoc. Prof., Dept. of Building Techn. and Struct. Engrg., University of Aalborg.

Ulfkjær, Brincker and Krenk (1990). In the present paper this model is presented using a linear softening relation and the model is validated by comparing with results from a numerical model.

Several general results are obtained. It is shown that the point on the load-displacement curve where the fictitious crack starts to develop, and the point where the real crack starts to grow always will correspond to the same bending moment, the points lying on each side of the peak point. Closed form solutions for the maximum size of the fracture zone and the minimum slope on the load-displacement curve are given. The last result is used for derivation of a general snap-back criterion depending only on beam geometry.

Basic Assumptions

The failure of a simply supported beam loaded in three point bending is modelled by assuming development of a single fictitious crack in the midsection of the beam.

In the FC-model material points on the crack extension path are assumed to be in one of three possible states: A) a linear elastic state, B) a fracture state where the material is softened, caused by cohesive forces in the fracture process zone and finally, C) a state of no stress transmission. In the fracture state the cracking process is described by a softening relation which relates stress normal to the cracked surface σ to the crack opening displacement, w (distance between the cracked surfaces)

$$\sigma = f(w) \cdot \dots \dots \dots (1)$$

where $f(\cdot)$ is a material function determined by uniaxial tensile tests, see Fig. 1. The area under the material function is termed the specific fracture energy, G_F , which is assumed to be a material constant, Elfgren (1989).

Usually the FC-model is combined with numerical methods like the finite element method Hillerborg et al. (1976) or a boundary element method like the substructure method introduced by Petersson (1981), and therefore no simple method of analysis is directly available.

Therefore, in this paper the model is further simplified by two additional assumptions: 1) the complex stress field around the crack is modelled by simple spring-action in an elastic layer around the crack, and outside the layer the deformations are modelled by beam theory 3) the softening relation is assumed to be linear.

The first assumption is characteristic of the model concept and cannot be changed without changing the whole idea of the model. The second assumption however is not inherent with the model and the linear softening relation might be changed to a Dugdale relation or another softening relation. Using the assumption of a linear softening relation however, the fracture energy is given by $G_F = \frac{1}{2} \sigma_u w_c$ where σ_u the ultimate tensile stress and w_c is the critical crack opening displacement, see Fig. 1. In the elastic layer only bending stresses are assumed to be present and the stress is assumed to depend linearly on the local elongation of the layer. Assuming a linear softening relation, the constitutive relation of the layer becomes a bi-linear relation between the axial stress σ and the elongation v , Fig. 2. On the ascending branch the elongation is linear elastic $v = v_e$ and no crack opening is present. The linear response is given by $v_e = \sigma h / E$ where h is the thickness of the layer, and E is Young's modulus. On the descending branch, however, the total deformation v consists of two contributions $v = v_e + w$, where w is the crack opening displacement. The peak point corresponds to the deformation $v = v_u$, and total fracture corresponds to $v = v_c$. Therefore, the critical crack opening

displacement w_c correspond to $w_c = v_c$.

To have a meaningful model it is necessary that the elastic layer is stable in displacement controlled loading corresponding to

$$v_u < v_c \dots \dots \dots (2)$$

In concrete fracture it is common to describe the material parameters and the beam size l in one parameter, the brittleness number, usually defined as $\sigma_u^2 l / G_F E$, Elfgren (1989). In the present case it is convenient to define the brittleness number as

$$B = \frac{\sigma_u^2 h}{2 G_F E} \dots \dots \dots (3)$$

whereby the stability condition (2) can be written

$$B < 1 \dots \dots \dots (4)$$

Thus, in this model the brittleness, B , number varies between zero corresponding to ideal ductile behaviour and one corresponding to ideal brittle behaviour. The thickness h of the elastic layer, is assumed to be proportional to the beam depth $h = kb$.

Solutions for Load-Displacement Curve

As a first approximation only rigid body displacement of the beam parts is assumed, Fig. 2.

The calculations are divided into three phases. Phase I): Before the tensile strength is reached in the tensile side of the beam, phase II): Development of a fictitious crack in the layer, and phase III): Crack propagation. The stress distribution in each phase of the fracture process is illustrated in Fig. 4.

In phase I a linear elastic constitutive relation is used for all parts of the layer $v_e = \sigma h / E$. By simple geometric considerations it is seen that $v_e = \varphi (b - 2y)$ where φ is the rotation, b is the beam depth and y is the vertical coordinate, Fig. 2. The neutral axis is at the mid-point of the beam corresponding to $y = b/2$. Instead of the bending moment M and the rotation φ it is convenient to introduce the dimensionless bending moment

$$\mu = M \frac{6}{\sigma_u b^2 t} \dots \dots \dots (5)$$

and the corresponding dimensionless displacement

$$\theta = \varphi \frac{bE}{h\sigma_u} = \varphi \frac{E}{k\sigma_u} \dots \dots \dots (6)$$

giving the simple load-displacement relation

$$\mu(\theta) = \theta \dots \dots \dots (7)$$

In the limit situation of phase I the stress for $y=0$ equals the tensile strength, and the dimensionless bending moment equals one. Thus, in phase I the load-displacement curve is a straight line between origo and $(\theta, \mu) = (1, 1)$, see Fig. 5.

In phase II the size of the elastic tensile zone is determined by simple geometrical considerations. When the fictitious crack develops, it is necessary to determine the crack

opening displacement. By assuming that the stress in the fictitious crack is equal to the stress in the elastic layer, the crack opening displacement becomes

$$w = \frac{2\varphi}{1-B}(a_f - y) \dots \dots \dots (8)$$

where a_f is the length of the fictitious crack. Thus, this corresponds to a linear crack profile. If the linear softening relation is expressed as

$$\sigma = \sigma_u \left(1 - \frac{w}{w_{fc}}\right) \dots \dots \dots (9)$$

then the length of the fictitious crack can be determined by combining (9) with the equilibrium condition (the resultant axial force equal to zero). The result reduces to

$$\alpha_f(\theta) = \frac{a_f}{b}(\theta) = 1 - B - \sqrt{(1-B)\left(\frac{1}{\theta} - B\right)} \dots \dots \dots (10)$$

The equivalent moment is determined by integrating the axial stresses

$$\mu(\theta) = \theta \left[\frac{2\alpha_f(\theta)^3}{1-B} - 6\alpha_f(\theta) + 4 \right] - 3 \dots \dots \dots (11)$$

In order to stay in phase II the crack opening displacement at the bottom of the beam must be smaller than the critical crack opening $w(0) < w_c$, which by use of (8), (10) and (11) can be reformulated as

$$\mu(\theta) > 1 \quad \text{or} \quad \theta < \theta_c \dots \dots \dots (12)$$

where

$$\theta_c = \frac{1 + \sqrt{B}}{2B} \dots \dots \dots (13)$$

Thus, during the development of the fictitious crack the moment increases from 1 to its ultimate value and then decreases again. When the moment reaches the value 1 at the descending branch corresponding to $\theta = \theta_c$ the real crack starts to grow, see Fig. 5. The real crack will therefore only propagate on the descending branch of the load displacement curve as found by Harder (1991).

In phase III the real crack starts to grow. The real crack length is termed a , see figure 4. The size of the elastic tensile zone is determined by the condition that $w(a + a_f) = w_u$. The size of the fictitious crack, a_f , is obtained by the condition $w(a) = w_c$ giving

$$\alpha_f = \frac{1}{2\theta} \frac{1-B}{B} \dots \dots \dots (14)$$

The crack length a is determined through the equilibrium condition that the resultant axial force is equal to zero

$$\alpha = \frac{a}{b} = 1 - \frac{\theta_c}{\theta} \dots \dots \dots (15)$$

As in phase II the dimensionless bending moment is determined by integrating the axial

stresses. The result is

$$\mu(\theta) = \left(\frac{\theta_c}{\theta} \right)^2 \dots \dots \dots (16)$$

When θ_c is suitably modified this result is general in the sense that it is valid for all softening relations. The results for the moment-rotation curve including only rigid body displacements of the beam parts are shown in Fig. 5.

Elastic deformations in the beam parts outside the elastic layer are taken into account by subtracting the elastic deformation $\mu(\theta)$ from the elastic layer leaving only deformations due to crack growth and adding the elastic deformations of the whole beam using a solution for a Timoshenko beam, Timoshenko S. (1955). The Timoshenko displacements are

$$\delta_e = \frac{Ml^2}{12EI} \beta(\lambda) \dots \dots \dots (17)$$

where EI is the bending stiffness of the beam, β is a factor describing the influence of shear $\beta = 1 + 2.85/\lambda^2 - 0.84/\lambda^3$, and λ is the slenderness ratio $\lambda = b/l$. Introducing the elastic rotation similar to equation (6)

$$\theta_e = 2 \frac{\delta_e}{l} \frac{bE}{h\sigma_u} \dots \dots \dots (18)$$

the relation (17) can be written in dimensionless form

$$\theta_e = \gamma \mu \dots \dots \dots (19)$$

where

$$\gamma = \frac{\beta(\lambda)}{3k\lambda} \dots \dots \dots (20)$$

and the total deformation is then given by subtracting the elastic deformation in the layer and the adding the deformations of the Timishenko beam

$$\theta_t = \theta - \mu(\theta) + \theta_e = \theta + (\gamma - 1)\mu(\theta) \dots \dots \dots (21)$$

Hence, the complete moment rotation curve is fully determined by the brittleness number B , and the slenderness λ .

Model Validation

In this section results from the analytical model are compared with results from a more detailed numerical model. The numerical model is based on the fictitious crack model and a linear softening relation.

The numerical results are obtained by the direct substructure method (DSS), Dahl and Brincker (1989). In the direct substructure method four-node elements and an element mesh with 21 nodes in the midsection were used.

Results for one beam geometry (slenderness ratio $\lambda = 8$) are compared at different brittleness levels in order to see how well the model predicts the load-displacement curve. It

is assumed that the size of the elastic layer is proportional to the beam depth $h = kb$ where the factor k is assumed to be 0.5. A beam geometry similar to the RILEM beam and material parameters corresponding to a normal strength concrete is chosen as standard beam, see table 1. With the chosen material parameters the maximum beam depth is according to (4) 888 mm corresponding to a scale factor of 8.88.

Table 1. Geometry and materials parameters for standard beam.

Beam Depth, b [mm]	100.0
Beam Width, t [mm]	100.0
Beam Length, L [mm]	800.0
Notch depth, a_i [mm]	0.0
Specific Fracture Energy, G_F [Nmm/mm ²]	0.100
Tensile Strength, σ_u [N/mm ²]	3.0
Modulus of Elasticity, E [N/mm ²]	20,000
Brittleness number, B	0.1125

In Fig. 6. a comparison is shown between the analytical model and the numerical results for the standard beam on 4 different size scales (0.25, 0.5, 1.0 and 3.0). It is observed that the shape of the moment-rotation curves is almost identical and that the model predicts the ultimate load quite well. However, in the analytical model the snap-back effect is more pronounced which implies that the analytical model is a little too brittle.

In Fig. 7 results for the size of the fictitious crack are compared. It is seen that the size of the fictitious crack calculated by the analytical model is slightly smaller than that calculated by the numerical method before the real crack starts to grow (the ascending branch of the curves) and larger at the descending branch. The small kinks on the numerical curve are due to the discretization made in the numerical model. With a larger number of nodes in the midsection these kinks would disappear. In Fig. 8 the real crack lengths for the two models are compared. It is seen that the real crack grows faster in the numerical model.

The peak loads, μ_{max} , predicted by the analytical and the numerical models are shown in log-log scale in figure 9. Since there is no stress singularity included in the two models there is no size effect beyond the critical size of the models. In the numerical model this limit will depend upon the material parameters and the number of nodes there are in the midsection (here the critical size scale is approximately 20).

The model is extended to notched beams as indicated in Fig. 11. The idea is to keep the width/depth ratio of the elastic layer by setting the width of the layer equal to k times the effective beam depth of the notched beam section $h = k(b-a_i)$, $k = 0.5$ where a_i is the depth of the notch. The modifications thus introduced imply that the brittleness number B for the layer is multiplied by a factor $(1-a_i/b)$. The total beam depth is still used in the formulas (5), (6) and (17) whereas the effective beam depth $b_e = b-a_i$ is used in all other formulas. Results for different notch depth's are shown in Fig. 12.

Comparing numerical results with results for the analytical model it can be concluded, that deviations are relatively small. The errors introduced by the elastic layer and the assumption

of wedge-like crack-opening is typically smaller than errors due to the simple linear softening relation, Brincker and Dahl (1989).

Size Effects Predicted by the Model

When the size of the beam changes, the stress distribution in the partially fractured mid-section changes and so does the shape of the load-displacement curve. In the following a few closed form solutions are given for these size effects predicted by the analytical model.

An important parameter describing the stress distribution in the partially fractured mid-section, is the maximum size $a_{f,max}$ of the fictitious crack.

Since $\partial a_f / \partial \theta > 0$ in phase II and $\partial a_f / \partial \theta < 0$ in phase III, a_f is largest at the end of phase II. Thus, the maximum size of the fictitious crack is found by combining eqs. (10) and (12)

$$a_{f,max} = b(1 - \sqrt{B}) \dots \dots \dots (22)$$

Thus, for small ductile beams the relative size of the fictitious crack is large and for large brittle beams the relative size of the fictitious crack approaches zero.

The way the load-displacement curve changes with size is more difficult to describe. One important parameter of the load-displacement curve is the peak load, μ_{max} . The peak load might be obtained from the condition $\partial \mu / \partial \theta_t = 0$. However, no simple expressions have been derived for this case.

Another key-parameter for the load-displacement curve is the maximum slope S on the descending branch. The slope is found by taking the derivative of eq. (21)

$$1 = \frac{\partial \theta}{\partial \mu} \frac{\partial \mu}{\partial \theta_t} + (\gamma - 1) \frac{\partial \mu}{\partial \theta_t} \dots \dots \dots (23)$$

from which

$$\frac{\partial \mu}{\partial \theta_t} = \left(\gamma - 1 + \frac{\partial \theta}{\partial \mu} \right)^{-1} \dots \dots \dots (24)$$

The steepest point on the descending branch of the load-displacement curve is at the transition from phase II to phase III, i.e. for $\theta = \theta_{cr}$. Thus, the minimum value of $\partial \theta / \partial \mu$ is found from eq. (16) and (13) which together with eq. (24) yield the results

$$S = \frac{4B}{1 + \sqrt{B} - 4(\gamma - 1)B} \dots \dots \dots (25)$$

The quantity S is a kind of brittleness number for the structure. The larger maximum slope on the descending branch, the more brittle the behaviour of the beam will be. The brittleness number varies between zero corresponding to ideal ductile behavior and infinity corresponding to the case where the maximum slope becomes infinite. If the point of infinity slope is exceeded, snap-back occurs, and the brittleness number S becomes meaningless. Thus, the brittleness number S only describes the brittleness of structures without snap-back on the load-displacement curve.

The maximum slope on the descending branch becomes infinite when the denominator in eq. (25) vanishes, i.e. when

$$1 + \sqrt{B} - 4(\gamma - 1)B = 0 \dots \dots \dots (26)$$

The solution to this equation defines a critical brittleness number for the elastic layer

$$B_{cr} = \left(\frac{1 + \sqrt{1 + 16(\gamma - 1)}}{8(\gamma - 1)} \right)^2 \dots \dots \dots (27)$$

If the brittleness number B of the layer is larger than the critical brittleness number B_{cr} then there is snap-back on the load-displacement curve. Otherwise there is no snap-back. For the standard beam the critical brittleness number is found as $B_{cr} = 0.069$ corresponding to a scale factor of 0.615. The case is illustrated in Fig. 10 where the results for the analytical model are shown for $B = B_{cr}$.

Conclusions

A simple model for calculation of load-displacement curves of notched and un-notched concrete beams in three point bending is presented. The results from the analytical model are compared to results from a numerical model based on the direct substructure method. Using the simple relation $h = kb$ where b is the depth of the notched or un-notched mid-section, the analytical model appears to give fine results.

The analytical model is described by a set of simple equations and, therefore, the calculation time is considerably less than the calculation time using a numerical model. Therefore, if a linear softening relation is acceptable, the model is well suited for estimation of material parameters from test results by regression.

Since the model takes both elastic and fracture energies into consideration, the model is able to predict both size effects and snap-back. However, the model has a limit depending on the brittleness modulus and is therefore not applicable to large brittle beams.

Acknowledgements

The financial support from the Danish Research Council is gratefully acknowledged.

Appendix I. References

- Bazant Z.P., and Oh, B.H. (1983), Crack Band Theory for Fracture of Concrete, *Materials and Structures*, 16, pp. 155-177.
- Blakey, F.A. and Beresford, F.D. (1962), Discussion of the Paper Kaplan M.F. Crack Propagation and the Fracture of Concrete, *JACI*, 58 (11), 591-610 (1961)., *JACI*, 59, 919-923.
- Brincker, R. and Dahl, H. (1989), On The Fictitious Crack Model of Concrete Fracture, *Magazine of Concrete Research*, 41, No. 147, pp.79-86.
- Chuang, T. and Mai, Y.W. (1989), Flexural Behavior of Strain-Softening Solids, *Int. J. Solids Structures*, Vol. 25, No. 12, pp. 1427-1443.
- Elfgren, L (1989), Fracture Mechanics of Concrete Structures - From Theory to Application, *Chapman and Hall*, RILEM Report.
- Glücklich, J. (1962), Discussion of the Paper Kaplan M.F. Crack Propagation and the Fracture of Concrete , *JACI*, 58 (11), 591-610 (1961).}, *JACI*, 59, 919-923.

- Harder, N.A. (1991), A Theorem on Brittleness, University of Aalborg, ISSN 0902-7513-R9126, pp. 1-17.
- Hillerborg, A., Modeer, M. and Petersson, P.E. (1976), Analysis of Crack Formation and Crack Growth in Concrete by Means of Fracture Mechanics and Finite Elements, *Cement and Concrete Research*, pp. 773-782.
- Irwin, G.R. (1962), Discussion of the Paper Kaplan, M.F.: Crack Propagation and the Fracture of Concrete, *JACI*, 58 (11), 591-610 (1961)., *JACI*, 59, 929.
- Jenq, Y.S and Shah, S.P. (1985), Two Parameter Fracture Model for Concrete, *Jour. Eng. Mech.*, ASCE, Vol. 111, no.10, pp. 1227-1240.
- Kaplan, M.F. (1961), Crack Propagation and the Fracture of Concrete, *Journal of the American Concrete Institute (JACI)*, 58 (11), pp. 591-610.
- Petersson, P.E. (1981), Crack Growth and Development of Fracture Zones in Plain Concrete and Similar Materials, *Division of Building Materials*, report TVBM-1006, pp.23-30.
- Planas, J., Elices, M. (1989), Asymptotic Analysis of the Development of a Cohesive Crack Zone in Mode I Loading for Arbitrary Softening Curves, *Proceedings of Fracture of Concrete and Rock* (S.P. Shah and S.E. Swartz, Editors), SEM-RILEM Conference. Houston p. 384.
- Timoshenko, S. (1955), *Strength of Materials, Part I, Elementary Theory and Problems*, Third edition, D. Van Nostrand Company Inc., New York, p. 174.
- Ulfkjær, J.P., Brincker, R. and Krenk, S. (1990), Analytical Model for Moment-Rotation Curves of Concrete Beams in Bending Fracture Behavior and Design of Materials and Structures, *Proceedings of the 8th European Conference on Fracture-ECF8* (Editor D. Firrao), Engineering Materials Advisory Services LTD, Vol. II pp.612-617.

Appendix II. Notation

The following symbols are used in this paper:

- a = crack length;
- a_f = fictitious crack length;
- B = brittleness modulus;
- b = beam depth;
- E = modulus of elasticity;
- $f(\cdot)$ = material function;
- G_F = specific fracture energy;
- h = thickness of elastic layer;
- I = moment of inertia;
- k = elasticity coefficient which determines the thickness of the elastic layer;
- l = beam length;
- M = cross-sectional moment;
- w = crack opening displacement;
- w_c = critical crack opening displacement;
- v = elongation of layer;
- v_c = critical elongation of layer;
- v_u = elongation of layer corresponding to the tensile strength;
- t = beam thickness;
- α = normalized crack length;

- α_f = normalized fictitious crack length;
- β = shear coefficient;
- γ = flexibility coefficient;
- φ = rotation of beam;
- θ = normalized rotation;
- θ_c = normalized rotation that separates phase II and III;
- λ = slenderness of the beam;
- μ = normalized cross-sectional moment;
- σ = axial stresses;
- σ_u = tensile strength;

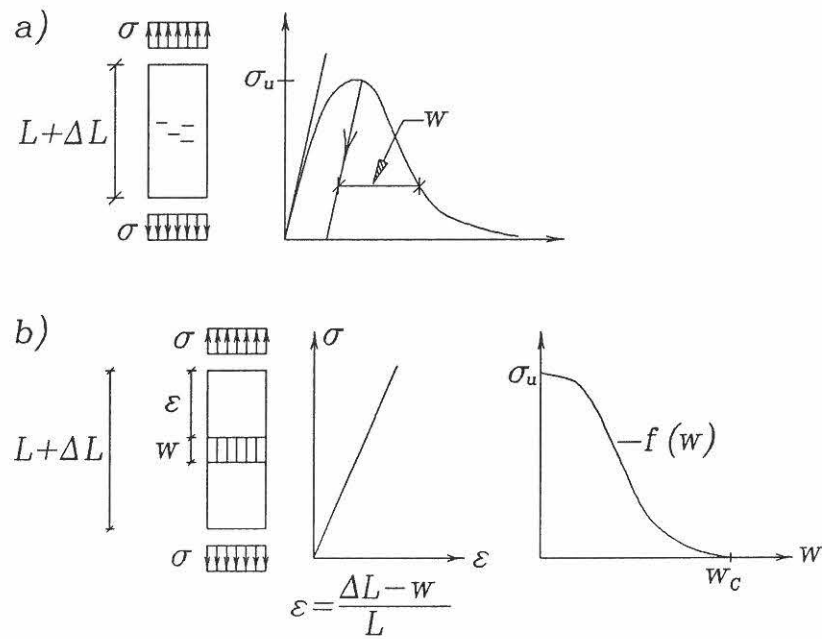


Fig. 1 a) Concrete rod subjected to uniaxial displacement controlled loading. b) In the fictitious crack model the displacement is divided into a stress-strain relation and a stress crack opening displacement relation.

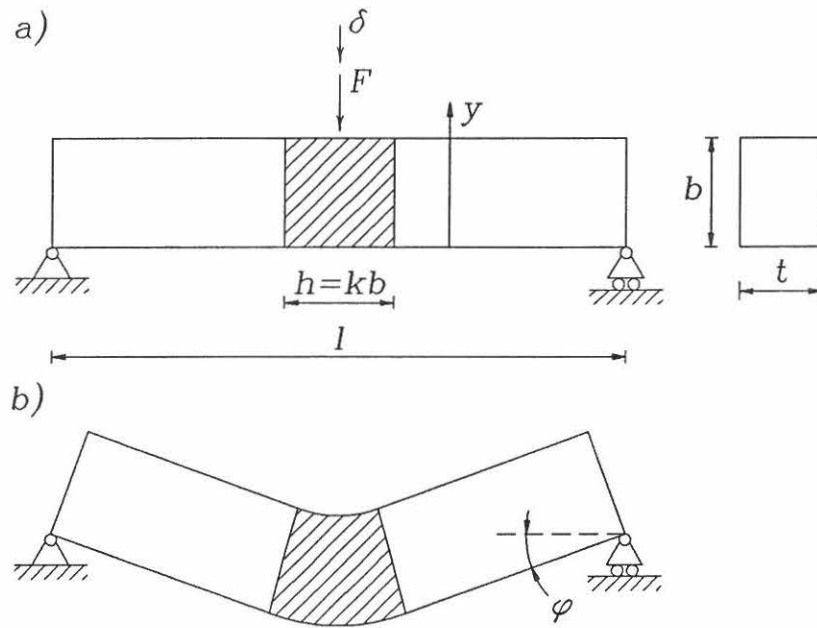


Fig. 2 a) The considered beam where the hatched area is the elastic layer. b) Deformed beam where only rigid body displacements are considered.

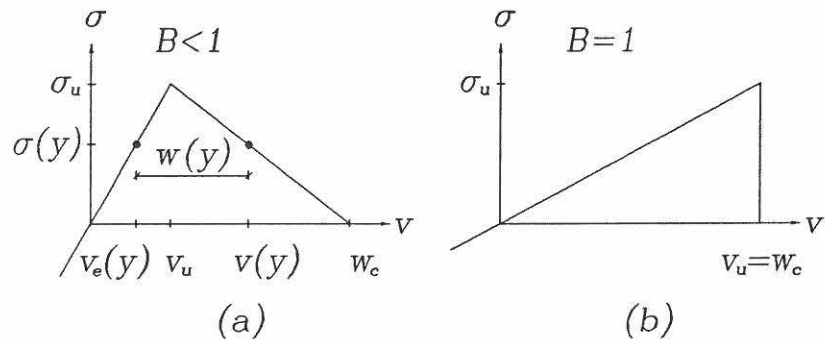


Fig. 3. Constitutive relation for the midsection of the layer a) When the layer is stable, $B < 1$. b) When the layer is unstable $B = 1$.

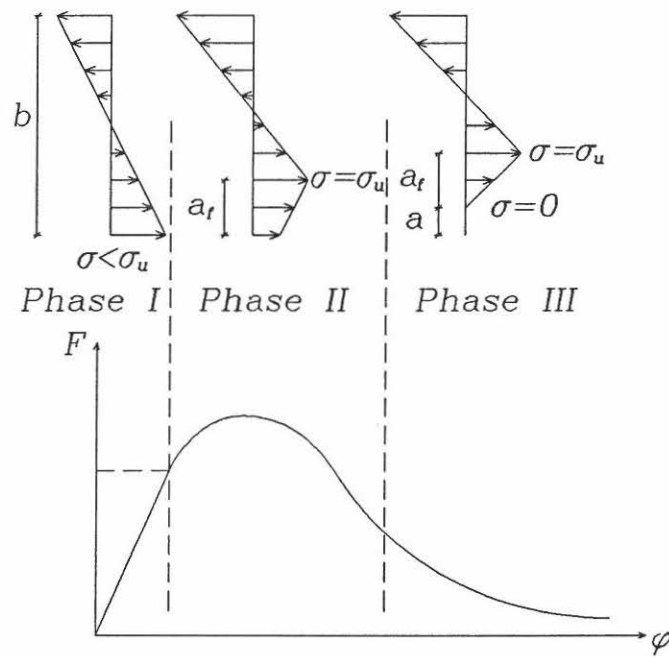


Fig. 4. The stress distributions of each phase a) Phase I where the stress distribution is elastic. b) Phase II where the fictitious crack is developed. c) Phase III where the real crack starts to grow. d) The load-displacement curve.

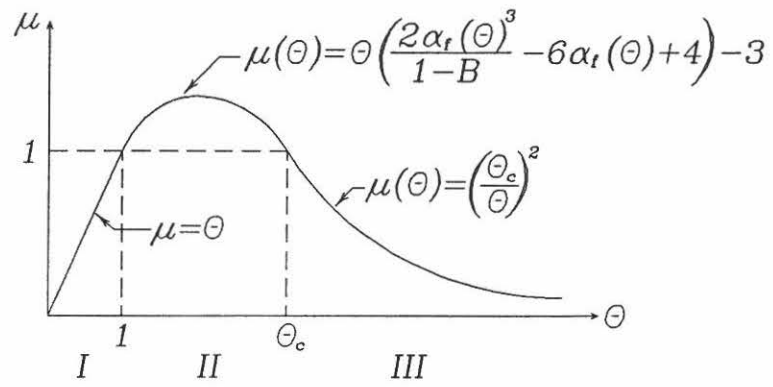


Fig. 5 The moment rotation curve of the beam when only rigid body displacements are considered.

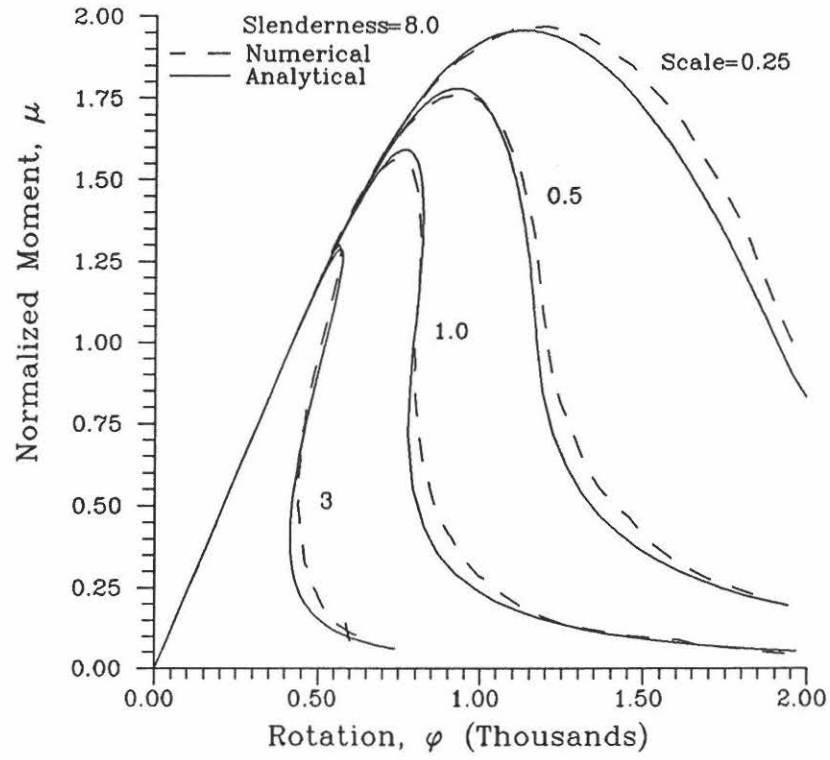


Fig. 6. Comparison between the analytical model and DSS using the standard beam at 4 different size scales.

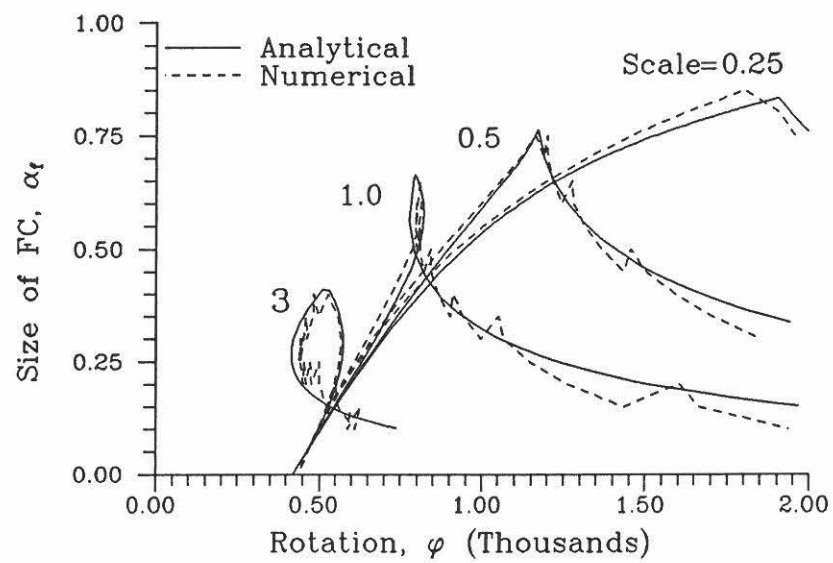


Fig. 7. Size of the fictitious crack for the analytical model and DSS. The loops are due to snap-back.

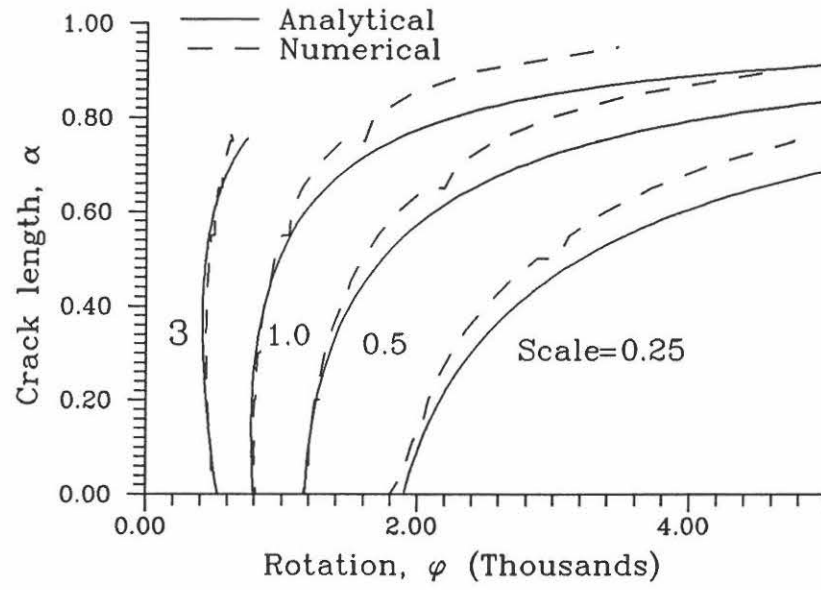


Fig. 8. Length of real crack for the analytical model and DSS.

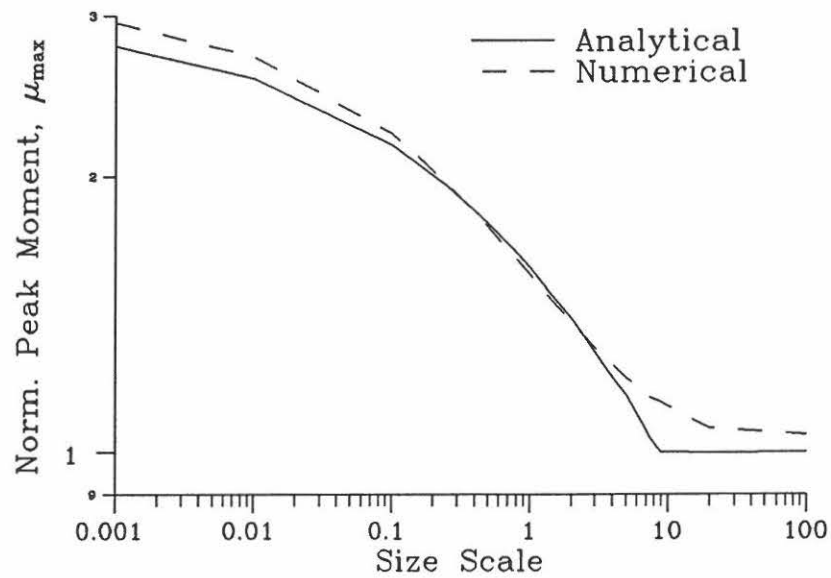


Fig. 9. Peak load at different size scales predicted by the model and by the DSS.

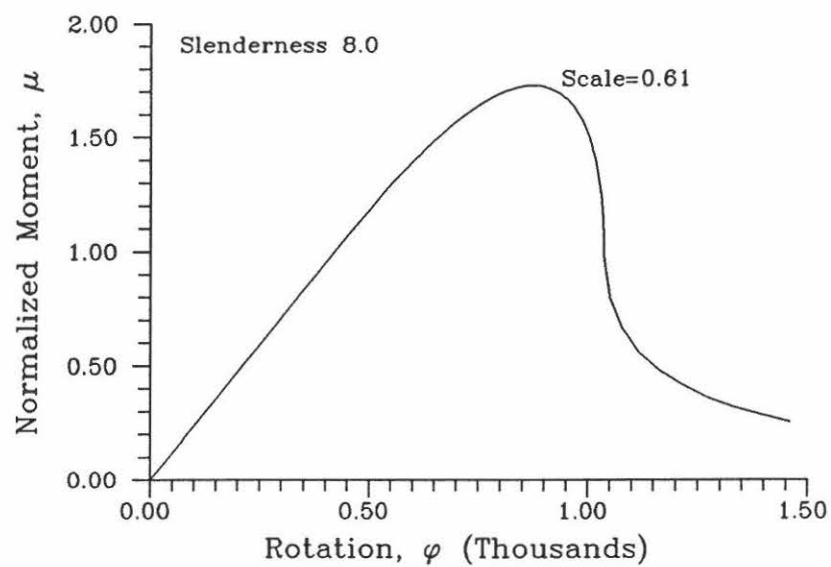


Fig. 10. Moment displacement curve for the beam on the critical size scale.

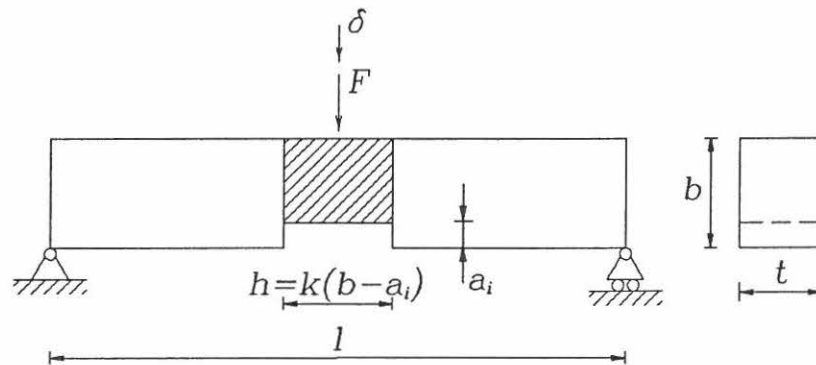


Fig. 11. Model of notched beam.

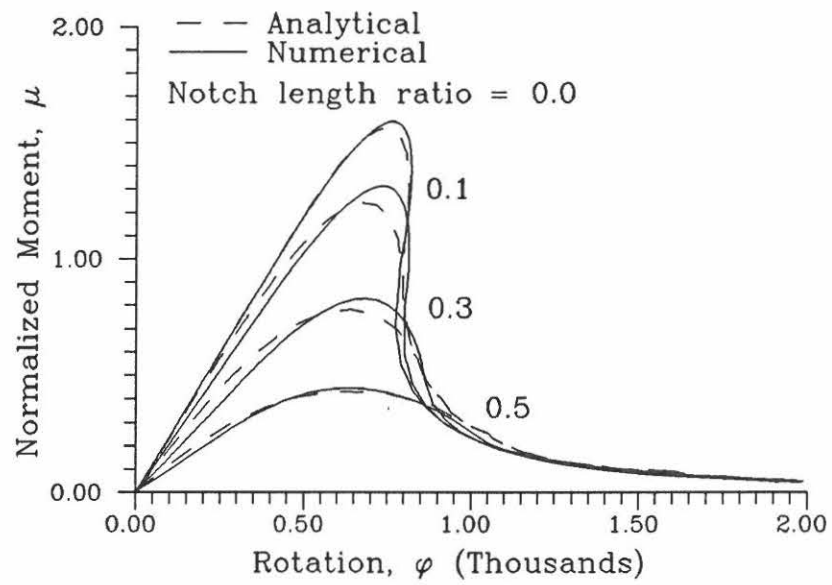


Fig. 12. Moment displacement curves for notched beams with three different notch depths.

FRACTURE AND DYNAMICS PAPERS

PAPER NO. 3: J. D. Sørensen: *PSSGP: Program for Simulation of Stationary Gaussian Processes*. ISSN 0902-7513 R8810.

PAPER NO. 4: Jakob Laigaard Jensen: *Dynamic Analysis of a Monopile Model*. ISSN 0902-7513 R8824.

PAPER NO. 5: Rune Brincker & Henrik Dahl: *On the Fictitious Crack Model of Concrete Fracture*. ISSN 0902-7513 R8830.

PAPER NO. 6: Lars Pilegaard Hansen: *Udmattelsesforsøg med St. 50-2, serie 1 - 2 - 3 - 4*. ISSN 0902-7513 R8813.

PAPER NO. 7: Lise Gansted: *Fatigue of Steel: State-of-the-Art Report*. ISSN 0902-7513 R8826.

PAPER NO. 8: P. H. Kirkegaard, I. Enevoldsen, J. D. Sørensen, R. Brincker: *Reliability Analysis of a Mono-Tower Platform*. ISSN 0902-7513 R8839.

PAPER NO. 9: P. H. Kirkegaard, J. D. Sørensen, R. Brincker: *Fatigue Analysis of a Mono-Tower Platform*. ISSN 0902-7513 R8840.

PAPER NO. 10: Jakob Laigaard Jensen: *System Identification1: ARMA Models*. ISSN 0902-7513 R8908.

PAPER NO. 11: Henrik Dahl & Rune Brincker: *Fracture Energy of High-Strength Concrete in Compression*. ISSN 0902-7513 R8919.

PAPER NO. 12: Lise Gansted, Rune Brincker & Lars Pilegaard Hansen: *Numerical Cumulative Damage: The FM-Model*. ISSN 0902-7513 R8920.

PAPER NO. 13: Lise Gansted: *Fatigue of Steel: Deterministic Loading on CT-Specimens*.

PAPER NO. 14: Jakob Laigaard Jensen, Rune Brincker & Anders Rytter: *Identification of Light Damping in Structures*. ISSN 0902-7513 R8928.

PAPER NO. 15: Anders Rytter, Jakob Laigaard Jensen & Lars Pilegaard Hansen: *System Identification from Output Measurements*. ISSN 0902-7513 R8929.

PAPER NO. 16: Jens Peder Ulfkjær: *Brud i beton - State-of-the-Art. 1. del, brudforløb og brudmodeller*. ISSN 0902-7513 R9001.

PAPER NO. 17: Jakob Laigaard Jensen: *Full-Scale Measurements of Offshore Platforms*. ISSN 0902-7513 R9002.

PAPER NO. 18: Jakob Laigaard Jensen, Rune Brincker & Anders Rytter: *Uncertainty of Modal Parameters Estimated by ARMA Models*. ISSN 0902-7513 R9006.

PAPER NO. 19: Rune Brincker: *Crack Tip Parameters for Growing Cracks in Linear Viscoelastic Materials*. ISSN 0902-7513 R9007.

PAPER NO. 20: Rune Brincker, Jakob L. Jensen & Steen Krenk: *Spectral Estimation by the Random Dec Technique*. ISSN 0902-7513 R9008.

FRACTURE AND DYNAMICS PAPERS

PAPER NO. 21: P. H. Kirkegaard, J. D. Sørensen & Rune Brincker: *Optimization of Measurements on Dynamically Sensitive Structures Using a Reliability Approach*. ISSN 0902-7513 R9009.

PAPER NO. 22: Jakob Laigaard Jensen: *System Identification of Offshore Platforms*. ISSN 0902-7513 R9011.

PAPER NO. 23: Janus Lyngbye & Rune Brincker: *Crack Length Detection by Digital Image Processing*. ISSN 0902-7513 R9018.

PAPER NO. 24: Jens Peder Ulfkjær, Rune Brincker & Steen Krenk: *Analytical Model for Complete Moment-Rotation Curves of Concrete Beams in bending*. ISSN 0902-7513 R9021.

PAPER NO. 25: Leo Thesbjerg: *Active Vibration Control of Civil Engineering Structures under Earthquake Excitation*. ISSN 0902-7513 R9027.

PAPER NO. 26: Rune Brincker, Steen Krenk & Jakob Laigaard Jensen: *Estimation of correlation Functions by the Random Dec Technique*. ISSN 0902-7513 R9028.

PAPER NO. 27: Jakob Laigaard Jensen, Poul Henning Kirkegaard & Rune Brincker: *Model and Wave Load Identification by ARMA Calibration*. ISSN 0902-7513 R9035.

PAPER NO. 28: Rune Brincker, Steen Krenk & Jakob Laigaard Jensen: *Estimation of Correlation Functions by the Random Decrement Technique*. ISSN 0902-7513 R9041.

PAPER NO. 29: Poul Henning Kirkegaard, John D. Sørensen & Rune Brincker: *Optimal Design of Measurement Programs for the Parameter Identification of Dynamic Systems*. ISSN 0902-7513 R9103.

PAPER NO. 30: L. Gansted & N. B. Sørensen: *Introduction to Fatigue and Fracture Mechanics*. ISSN 0902-7513 R9104.

PAPER NO. 31: R. Brincker, A. Rytter & S. Krenk: *Non-Parametric Estimation of Correlation Functions*. ISSN 0902-7513 R9120.

PAPER NO. 32: R. Brincker, P. H. Kirkegaard & A. Rytter: *Identification of System Parameters by the Random Decrement Technique*. ISSN 0902-7513 R9121.

PAPER NO. 33: A. Rytter, R. Brincker & L. Pilegaard Hansen: *Detection of Fatigue Damage in a Steel Member*. ISSN 0902-7513 R9138.

PAPER NO. 34: J. P. Ulfkjær, S. Krenk & R. Brincker: *Analytical Model for Fictitious Crack Propagation in Concrete Beams*. ISSN 0902-7513 R9206.

Department of Building Technology and Structural Engineering
The University of Aalborg, Sohngaardsholmsvej 57, DK 9000 Aalborg
Telephone: 45 98 15 85 22 Telefax: 45 98 14 82 43